JOURNAL OF DIFFERENTIAL EQUATIONS 158, 48–78 (1999)
Article ID jdeq.1999.3641, available online at http://www.idealibrary.com on IDEAL®

Uniqueness and Stability of Periodic Bursting Solutions

Euiwoo Lee

Department of Mathematics, Soongsil University, Seoul, Korea

and

David Terman

Department of Mathematics, Ohio State University, 231 West 18th Avenue, Columbus, Ohio 43210-1174

Received March 19, 1998; revised January 19, 1999

A detailed analysis of so-called square bursting oscillators is given. An interesting feature of these models is that the bursting solution need not be unique or stable for arbitrarily small values of a singular perturbation parameter. This is a global phenomenon due to interactions between a homoclinic orbit and other invariant manifolds. Using geometric singular perturbation methods we characterize the set of parameters for which the bursting solution is uniquely determined and asymptotically stable. © 1999 Academic Press

1. INTRODUCTION

Neurons and other excitable cells often exhibit bursting oscillations; this behavior is characterized by a silent phase of near steady state resting behavior and an active phase of rapid, spike-like oscillations as shown in Fig. 1. Examples of biological systems which display bursting oscillations include the Aplysia R-15 neuron, insulin secreting pancreatic beta cells, and neurons in the hippocampus, cortex and thalamus. For a review, see [38]. There are several different classes of bursting oscillations and there has been considerable effort in trying to characterize the underlying (mathematical as well as biological) mechanisms responsible for these oscillations [4, 27, 29, 31].

Mathematical models for bursting oscillations often display a rich structure of dynamic behavior [7, 35, 36]. Besides periodic bursting oscillations, these systems may exhibit other types of periodic solutions, such as continuous spiking, as well as more exotic behavior including chaotic dynamics. The models contain multiple time scales and this often leads to very interesting issues related to the theory of singular perturbations. For

0022-0396/99 $30.00

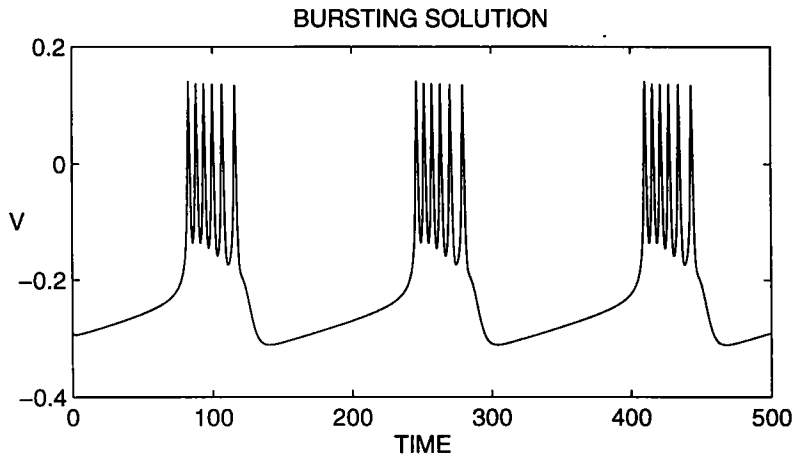

FIG. 1. An example of a bursting solution. The solution is computed using the equations in the Appendix.

example, homoclinic orbits usually play an important role in the dynamics; the active phase of rapid oscillations may either begin or end (or both) as a slow trajectory crosses a homoclinic point. It is at this point that many standard singular perturbation theories break down, so more delicate analysis is required. Moreover, the homoclinic orbits are often directly responsible for the generation of chaotic dynamics [35, 36].

In this paper, we give a detailed mathematical analysis of one class of model for bursting oscillations; this is the so-called square burster [26, 27]. The existence of periodic bursting solutions was proven in [35]. However, an interesting feature of these models is that the bursting solution need not always be unique or stable. For example, the number of spikes per burst will increase as the singular perturbation parameter ε decreases. The analysis in [35] demonstrated that these transitions can be quite complicated. In particular, the bursting solution may not be uniquely determined for those values of ε for which the transitions take place. For each positive integer n there corresponds a range of values for ε during which the model makes a transition from n to $n+1$ spikes per burst. These ranges of parameter values accumulate onto $\varepsilon = 0$ as $n \to \infty$. Hence, there is an infinite collection of parameter ranges for which the model may exhibit chaotic bursting behavior.

Here we characterize the set of parameters for which the bursting solution is uniquely determined; in this case the solutions must also be stable. Our general approach is straightforward; we determine when a certain flow-defined return map gives rise to a uniform contraction. However, in order to analyze the return map, we must carefully follow trajectories as they pass through different regions of phase space. These regions

correspond to different types of solutions to the fast subsystem in which the singular perturbation parameter is set equal to zero. The four primary regions are: (1) a branch of periodic solutions corresponding to the active phase of rapid spikes, (2) a branch of steady solutions corresponding to the silent phase, (3) a junction point where the transition between the silent and active phases takes place, and (4) a homoclinic orbit where the active phase terminates. The full return map is the composition of four separate flow-defined maps; each one of these determines the behavior of trajectories as they pass near one of the four regions of phase space. The analysis of each of these maps requires different tools from the geometric theories of dynamical systems and singular perturbations. For example, in order to understand the behavior of solutions near the branch of periodic orbits, we apply Fenichel's theory [13]. The analysis becomes especially delicate since we will need to understand how trajectories near the homoclinic orbit interact with a Fenichel fibration of the branch of periodic orbits.

An outline of the paper is the following. In Section 2, we formally present the model and then demonstrate why one should intuitively expect this model to exhibit bursting oscillations. The main result is stated in Section 3 where we also define the return map and give a more detailed outline of the proof. In Section 4, we analyze each separate portion of the flow. This information is put together in Section 5 where we complete the proof of the main theorem.

2. GEOMETRIC MODEL

2.1. *Assumptions on the Geometric Model*

The analytic framework we develop is quite general, so instead of restricting our attention to one specific model, we consider a general system of the form

$$\begin{aligned} v' &= f_1(v, w, y) \\ w' &= f_2(v, w, y) \\ y' &= \varepsilon g(v, w, y). \end{aligned} \tag{2.1}$$

Here f_1, f_2, and g are sufficiently smooth (say C^3) functions and ε is a small singular perturbation parameter. If $\varepsilon = 0$, then y is constant, and we can consider y to be a parameter in the first two equations of (2.1). We refer to these equations (with y constant) as the fast system (FS). We refer to the last equation in (2.1) as the slow equation.

We now discuss the assumptions needed so that (2.1) exhibits bursting oscillations. These conditions are geometric in the sense that we make assumptions on the nature of the fixed points, periodic and other bounded

solutions of (FS) and the slow equation. Most of these conditions are straightforward to verify for a specific model using numerics. Some conditions are technical; however, all of the more technical assumptions are quite natural. An example of a specific set of equations which satisfy these assumptions is given in the Appendix.

We assume that the set of fixed points of (FS) consists of an "S-shaped" curve, denoted by $\mathscr{S}$, as shown in Fig. 2. That is, there exist $y_\lambda < y_\rho$ such that if $y < y_\lambda$ or $y > y_\rho$, then (FS) has exactly one fixed point, while if $y_\lambda < y < y_\rho$ then (FS) has precisely three fixed points. We assume that the lower branch, denoted by $\mathscr{L}$, consists of fixed points which are stable as solutions of (FS) and the middle branch consists of fixed points which are saddles. See also Fig. 3.

We further assume that there exists a one parameter family of periodic solutions of (FS) as shown in Fig. 2. This branch, denoted by $\mathscr{P}$, surrounds a portion of the upper branch of fixed points and terminates at a solution which is homoclinic to one of the fixed points on the middle branch. We denote this homoclinic point by $p_h = (v_h, w_h, y_h)$.

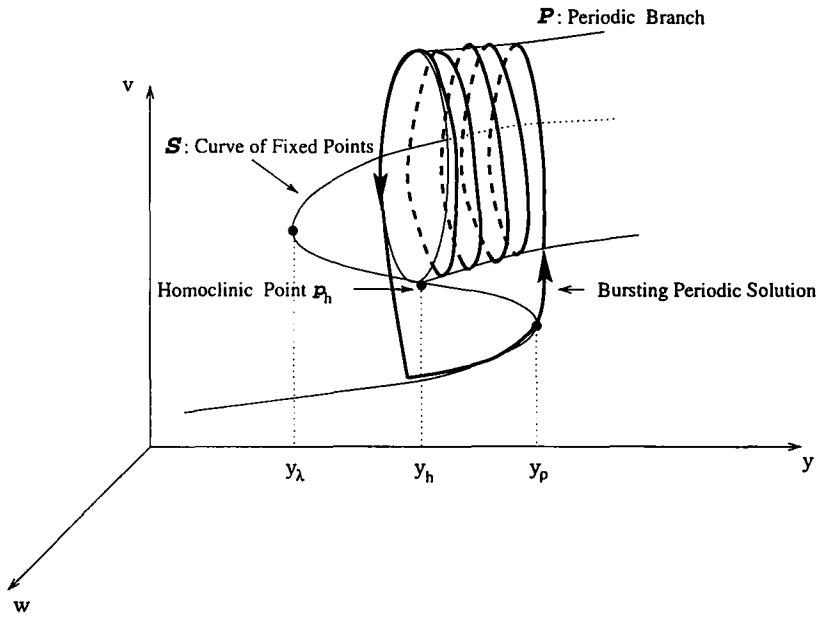

FIG. 2. Geometric model for bursting. The fast system has an S-shaped curve of fixed points and a branch of stable periodic solutions. The bursting solution passes near the lower branch of fixed points in the silent phase and passes near the periodic branch in the active phase.

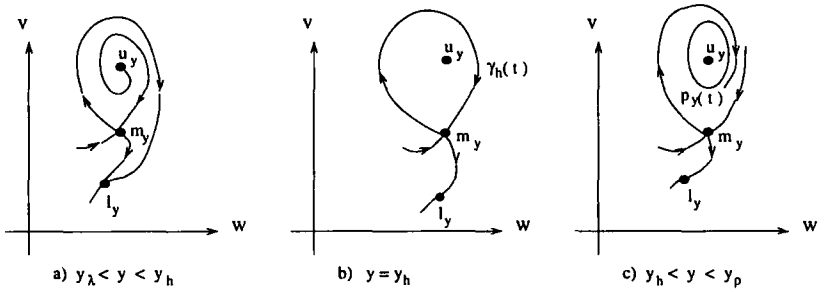

FIG. 3. The phase plane of (FS) for different values of y. For each $y \in (y_\lambda, y_p)$, one of the two trajectories in the unstable manifold of the fixed point along the middle branch approaches the stable fixed point on the lower branch. If $y > y_h$, then the other trajectory approaches the periodic solution; while, if $y < y_h$, then it ultimately approaches the lower stable fixed point.

Our next assumption is concerned with the $y-$nullsurface, $\mathcal{N} \equiv \{g = 0\}$. We assume that this defines a smooth surface which intersects the curve $\mathcal{S}$ at a unique point which lies below p_h. We further assume that $g > 0$ below $\mathcal{N}$, $g < 0$ above $\mathcal{N}$, and $\mathcal{N} \cap \mathcal{P} = \varnothing$.

We now state the more technical assumptions required for our analysis. The first technical assumption is that the homoclinic orbit arises from the transverse intersection of the two manifolds formed by taking the unions of the stable and unstable trajectories to the fixed points along the middle branch. A more analytic statement of this assumption is given in Subsection 4.3. The second technical assumption is concerned with the right knee. We assume that this knee is nondegenerate in some (obvious) sense. The precise condition is stated in Subsection 4.2. We next consider the lower branch of fixed points. We have already assumed that each of these fixed points is stable as a solution of (FS). We further assume that each is hyperbolic; that is, the linearization of (FS) about each fixed point has both eigenvalues with strictly negative real parts. We also need to assume that the manifold $\mathcal{P}$ is normally hyperbolic [10, 11]. The final assumption is that the set of solutions of (FS) considered so far represents all the bounded solutions of (FS). That is, every solution of (FS) approaches in forward time either one of the fixed points along $\mathcal{S}$, one of the periodic solutions along $\mathcal{P}$, or the homoclinic orbit.

2.2. *Bursting Solution*

It is easy to understand why the system (2.1) will give rise to a bursting solution. Here we give a heuristic description of how this solution behaves in phase space. Our description follows [26] and the trajectory is shown in Fig. 2.

Assume that ε is small, but positive. We start the trajectory near the lower branch. Because the lower branch consists of stable fixed points of (FS), the trajectory will quickly approach a small neighborhood of the lower branch. Now $g > 0$ near the lower branch. The solution must therefore track near the lower branch moving towards the right knee. This continues until the slow dynamics pushes the trajectory past the right knee. The trajectory is then attracted to near one of the periodic solutions along $\mathscr{P}$. This corresponds to the jump-up from the silent phase to the active phase. The fast spike-like oscillations of the bursting solution corresponds to the trajectory passing near and around $\mathscr{P}$. The slow dynamics now force the orbit to move slowly to the left. This continues until the trajectory passes near the homoclinic orbit of (FS). Once past this homoclinic orbit, the trajectory must eventually fall back to the silent phase. This completes one cycle of the bursting solution.

As we shall see, this informal description for the bursting solution can be easily justified, except for the portion of the trajectory near the homoclinic orbit. It requires delicate analysis in order to fully understand the passage near the homoclinic orbit and the mechanism for jumping down to the silent phase. This will turn out to be the key to understanding when the bursting solution is uniquely determined. In the next section we consider this in detail.

2.3. *When Do Trajectories Jump Down?*

In order to understand when the bursting solution jumps down to the silent phase, we need to consider the stable and unstable manifolds of the fixed points of (FS) along the middle branch. Note that there are two trajectories in the unstable manifold of each of these fixed points. See Fig. 3. One of these evolves towards the active phase, looping around the upper branch. If $y > y_h$, then this trajectory approaches one of the periodic solutions along $\mathscr{P}$, while if $y < y_h$, then it ultimately approaches a stable fixed point along the lower branch. The other unstable trajectory evolves directly towards the silent phase and approaches the stable fixed points along the lower branch.

Now the stable manifolds to the fixed points along the middle branch separate the two unstable manifolds. Hence, if a trajectory lies close to the middle branch, it will either give rise to a spike or jump down to the silent phase depending on which side of the stable manifold it lies on.

What we have described so far holds for $\varepsilon = 0$, however this all carries over for small $\varepsilon > 0$. To make this more precise, let W_0^s and W_0^u be the union of all the stable and unstable manifolds to the fixed points along the middle branch when $\varepsilon = 0$. (We must actually exclude a small neighborhoods of the left and right knees.) These are both smooth, two dimensional, invariant manifolds. For $\varepsilon > 0$, these manifolds perturb to

manifolds W^s_ε and W^u_ε (see [10]). These manifolds are both smooth, two-dimensional, invariant, and lie a C^1-distance $O(\varepsilon)$ close to W^s_0 and W^u_0 near the middle branch. If we let $W^c_\varepsilon = W^s_\varepsilon \cap W^u_\varepsilon$, then W^c_ε, W^s_ε, and W^u_ε are the center, center-stable, and center-unstable manifolds corresponding to the middle branch, respectively.

As before, W^s_ε divides W^u_ε into two pieces; one piece 'points' towards the active phase, while the other piece 'points' towards the silent phase. Hence, a trajectory near the middle branch may give rise to another spike or jump down depending on which side of W^s_ε it lies on.

We now discuss the significance of this to the bursting solutions. We start the bursting solution in the active phase near the branch of periodic orbits $\mathscr{P}$. It will then give rise to spikes as it tracks near $\mathscr{P}$ moving slowly to the left. As the orbit approaches the homoclinic orbit, it passes closer to the middle branch. As long as it keeps spiking, the orbit must lie on the "jump-up" side of W^s_ε. Eventually, however, the orbit will cross to the other side of W^s_ε. It is then that the orbit must jump down to the silent phase.

It is possible for the orbit to actually lie precisely on W^s_ε and it is important to understand the fate of these trajectories. As shown in Fig. 4, these orbits must track close to the middle branch (actually W^c_ε) slowly moving to the left. The orbit eventually jumps down near the left knee. Note that if we start very close to W^s_ε, then the trajectory will track close to the middle branch for some finite distance before it either jumps up or jumps down. If the bursting solution behaves in this way, then it will not behave like the 'typical' bursting solution, as described in Section 2.2. It is precisely

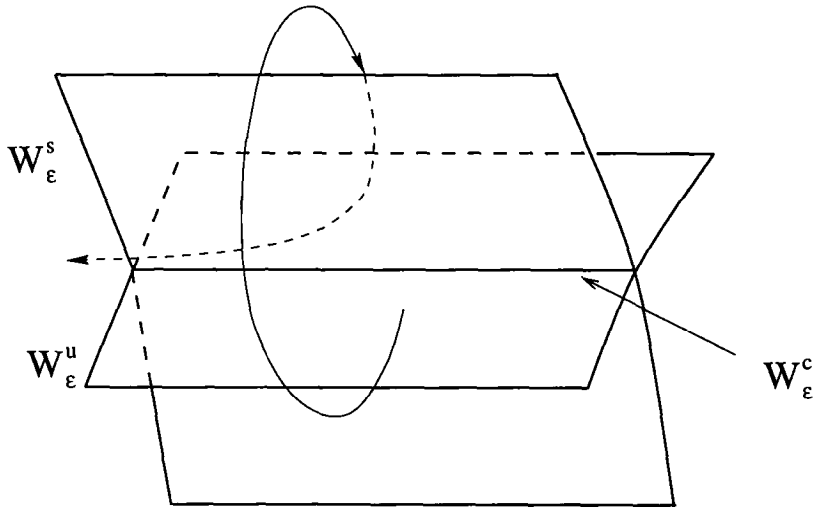

FIG. 4. The mechanism explaining why the uniqueness of bursting solutions may be destroyed. If an orbit lies very close to W^s_ε, then it tracks close to the middle branch for some finite distance.

this mechanism (lying close to W^s_ε) which can destroy the uniqueness and stability of the bursting solution. Hence, in order to determine whether the bursting solution is uniquely determined, we must estimate how close it passes to W^s_ε.

3. MAIN RESULT AND GEOMETRICAL ASPECTS OF THE PROOF

3.1. *Main Result*

We now state our main result. It characterizes the range of values of ε for which the periodic bursting solution is uniquely determined. We note that it is much easier to prove the existence of such solutions for all ε sufficiently small. This will also follow from the analysis.

THEOREM 3.1. *The periodic bursting solution is uniquely determined and asymptotically stable for all values of* $\varepsilon > 0$ *sufficiently small except for those in a set of the form* $\bigcup_{i=1}^{\infty} (\varepsilon_i - \delta_i, \varepsilon_i + \delta_i)$. *The* ε_i *and* δ_i *can be chosen so that* $\lim_{i \to \infty} \varepsilon_i = 0$. *Moreover,*

$$\varepsilon_i - \varepsilon_{i+1} > C_1 \varepsilon_i^2 \qquad \text{and} \qquad \delta_i \leqslant C_2 e^{-k/\varepsilon_i}$$

for some positive constants C_1, C_2, *and* k.

3.2. *Return Map and Outline of the Proof*

We prove the theorem by constructing a two dimensional section Σ transverse to the flow defined by (2.1) and then considering the return map from Σ back into Σ. We denote this map by π_ε. We prove uniqueness and stability of a bursting solution by showing that this map is a uniform contraction. Here we will outline some of the ideas needed in showing that the return map is a contraction over most values of ε, sufficiently small. These ideas will help motivate the analysis that follows.

We choose Σ so that it lies just above the right knee, as shown in Fig. 5. Hence, trajectories cross Σ transversely as they jump up to the active phase. The distance between Σ to the right knee is assumed to be small, but still independent of ε.

In order to determine when the return map is a contraction, we write it as the composition of several other maps; these maps correspond to the different pieces of the trajectories as they move around in phase space. The different pieces are:

(P1) the jump up

(P2) tracking near the branch of periodic solutions $\mathscr{P}$

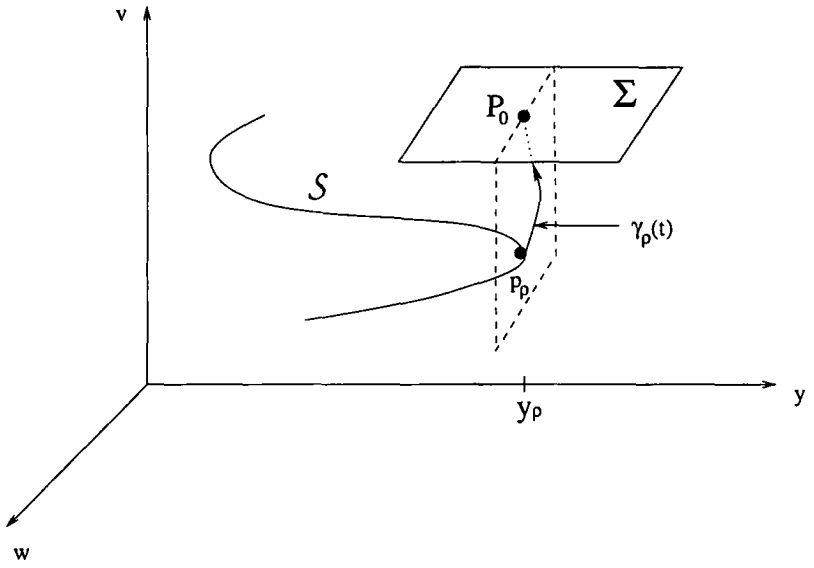

FIG. 5. The two-dimensional section Σ above the right knee. The Poincare return map π_ε is from Σ back to itself. As known in Subsection 4.2, there is a unique trajectory $\gamma_\rho(t)$ which approaches p_ρ as $t \to -\infty$.

(P3) motion near the homoclinic orbit and interaction with the middle branch

(P4) the jump down

(P5) tracking near the lower branch

(P6) passing near the right knee.

We need to estimate the amount of expansion or contraction induced by each of these pieces of the flow. We note that there will be a huge amount of contraction as trajectories pass near the lower branch. This contraction is so large that trajectories will enter an $O(e^{-k_0/\varepsilon})$ neighborhood of the lower branch. This contraction will easily dominate any possible expansion that can occur over the pieces (P1), (P2), (P4), or (P6). Hence, the only possible expansion that can ultimately destroy the uniform contraction of the entire map π_ε must occur during the piece labeled (P3). It will, in fact, be possible for exponential expansion to occur as the trajectories pass near the middle branch, just before they jump down to the silent phase. This is of course consistent with the discussion in the preceding section.

In order to obtain uniqueness, we must somehow avoid W^s_ε, the center-stable manifold of the middle branch. If it were true that W^s_ε and Σ had empty intersection, then there would be no problem with proving uniform contraction; however, as we shall see, this can never be the case. What may be true, however, is that W^s_ε has empty intersection with the range of the return map π_ε. We denote this range as $\Sigma^\varepsilon_1 \equiv \pi_\varepsilon(\Sigma)$. If this intersection is empty, then we will be able to obtain uniform contraction by restricting π_ε to Σ^ε_1.

We can now outline our strategy for proving the theorem. We shall consider two subsets of Σ. The first one is Σ^ε_1, the range of π_ε. For the second subset, we consider W^s_ε and follow it backwards by the flow until it intersects Σ. Denote this set by $\hat{\Sigma}^\varepsilon_2$. Our analysis will show that this set consists of a large number of curves in Σ as shown in Fig. 6. The number of such curves is asymptotically $O(1/\varepsilon)$. We then let Σ^ε_2 be a small neighborhood of $\hat{\Sigma}^\varepsilon_2$. This is a (large) number of narrow strips. Uniform contraction will follow if we can show that $\Sigma^\varepsilon_1 \cap \Sigma^\varepsilon_2 = \varnothing$.

In the analysis, we will need to estimate the size of Σ^ε_1 and choose each strip in Σ^ε_2 sufficiently narrow. We will also have to consider how these sets change with respect to ε. A key ingredient in the analysis will be that both of these sets change their positions as ε is varied, but the speed at which they move is different. For most values of ε, Σ^ε_1 and Σ^ε_2 have empty intersection. However, as ε varies, Σ^ε_1 'passes through' Σ^ε_2. This corresponds to the bursting solution either gaining or losing a spike in each of its bursts. For these values of the parameters, the bursting solution may not be uniquely determined.

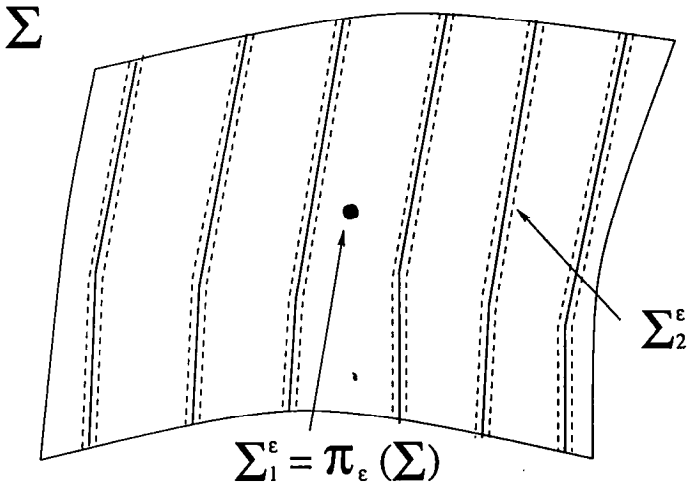

FIG. 6. Two subsets of Σ. The set Σ^ε_1 is the range of π_ε and the set Σ^ε_2 is a small neighborhood of $\hat{\Sigma}^\varepsilon_2$. The return map π_ε is a uniform contraction if $\Sigma^\varepsilon_1 \cap \Sigma^\varepsilon_2 = \varnothing$.

4. PIECES OF THE FLOW

We now describe the information we need concerning each piece of the flow. This information is then put together in the next section where we complete the proof of the theorem.

4.1. *Lower Branch*

The information we need concerning the flow near the lower branch follows from the geometric theory of Fenichel [13]. In this discussion, we only consider the portion of $\mathscr{L}$ bounded away from the right knee. Then $\mathscr{L}$ perturbs to a smooth invariant manifold $\mathscr{L}_\varepsilon$. Note that $\mathscr{L}_\varepsilon$ is only unique up to exponentially small terms. The distance from $\mathscr{L}$ to $\mathscr{L}_\varepsilon$ is $O(\varepsilon)$. Moreover, trajectories are attracted to $\mathscr{L}_\varepsilon$ at an exponential rate. An immediate consequence of this result is the following. Let Σ_ρ be a local section transverse to $\mathscr{L}$. We assume that the distance from Σ_ρ to the right knee is small but still independent of ε. See Fig. 7. Let p and q be two points which lie near $\mathscr{L}$ but are bounded away from Σ_ρ. The solutions of (2.1) which begin at p and q must cross Σ_ρ. We denote these points by P_ε^0 and Q_ε^0. Then

$$|P_\varepsilon^0 - Q_\varepsilon^0| < e^{-k_0/\varepsilon}\,|p-q| \tag{4.1}$$

for some constant $k_0 > 0$ that does not depend on ε. Hence, there is a huge amount of compression near the lower branch.

This result has an immediate consequence for the bursting solutions. Let $\bar{P}_\varepsilon^0$ be the point where $\mathscr{L}_\varepsilon$ intersects Σ_ρ. This is shown in Fig. 7. Now let p be any point in Σ. The solution of (2.1) which is initially at p must eventually jump down to the silent phase at some point bounded away from the right knee. Hence, this solution must cross Σ_ρ at some point which we denote by P_ε^0. It follows from (4.1) that we can choose $c > 0$ so that

$$|P_\varepsilon^0 - \bar{P}_\varepsilon^0| < ce^{-k_0/\varepsilon}. \tag{4.2}$$

Hence, the entire set Σ is mapped by the flow onto a very small subset of Σ_ρ.

4.2. *Right Knee*

We first state the precise assumptions required on the right knee (or the *junction point*). In order to state these conditions, it will be useful to introduce some notation. Denote the right knee by $p_\rho \equiv (v_\rho, w_\rho, y_\rho)$. Let $X = (v, w)$ be the fast variables and let $F = (f_1, f_2)$. Now the curve of fixed points is, by definition, given by $\mathscr{S} \equiv \{(X, y): F(X, y) = 0\}$. In order for $p_\rho \in \mathscr{S}$ to be a junction point, we assume that $A \equiv D_X F(p_\rho)$ has one

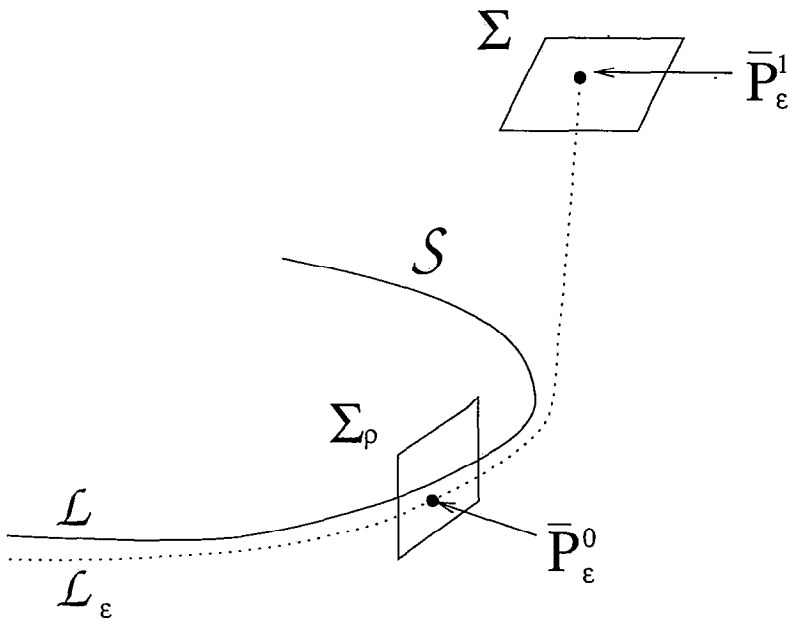

FIG. 7. The section Σ_ρ at the lower branch. The points $\bar{P}^0_\varepsilon$ and $\bar{P}^1_\varepsilon$ are where $\mathcal{L}_\varepsilon$ intersects Σ_ρ and Σ, respectively.

negative eigenvalue and one zero eigenvalue. We need to also assume that p_ρ is nondegenerate in the following sense: Let η be the eigenvector corresponding to the zero eigenvalue of A and denote the eigenvector corresponding to the zero eigenvalue of the transpose of A by ζ. We assume that $\langle \zeta, D_y F(p_\rho)\rangle \neq 0$ and $\langle \zeta, D_X^2 F(p_\rho)(\eta, \eta)\rangle \neq 0$. From the last assumption, there is a unique trajectory $\gamma_\rho(t)$ of (FS) which approaches p_ρ as $t \to -\infty$. Let P_0 be the point where this trajectory crosses Σ. See Fig. 5.

We now discuss the information that will be needed concerning the flow near the right knee. Here we only state the results; their proofs can be found in [20]. Let $\bar{P}^0_\varepsilon$ be as in the preceding section and let $\bar{P}^1_\varepsilon = (\bar{v}^1_\varepsilon, \bar{w}^1_\varepsilon, \bar{y}^1_\varepsilon)$ be the point where the solution of (2.1) which begins at $\bar{P}^0_\varepsilon$ crosses Σ. Then there exist positive constants c_1 and c_2 such that

$$c_1 \varepsilon^{2/3} < \bar{y}^1_\varepsilon - y_\rho < c_2 \varepsilon^{2/3} \qquad \text{and} \qquad \bar{P}^1_\varepsilon \to P_0 \quad \text{as} \quad \varepsilon \to 0. \tag{4.3}$$

Let P^1_ε and Q^1_ε be the points where the solutions of (2.1) which pass through P^0_ε and Q^0_ε cross Σ. Then

$$|P^1_\varepsilon - Q^1_\varepsilon| < e^{-k_1/\varepsilon}|p - q| \tag{4.4}$$

for some positive $k_1 < k_0$. From (4.2), this implies that c_1' and c_2' can be chosen so that if $p \in \Sigma$ and $\pi_\varepsilon(p) = (v_\varepsilon(p), w_\varepsilon(p), y_\varepsilon(p))$, then

$$|\pi_\varepsilon(p) - \bar{P}_\varepsilon^1| = O(e^{-k_1/\varepsilon}) \qquad \text{and} \qquad c_1' \varepsilon^{2/3} < |y_\varepsilon(p) - y_p| < c_2' \varepsilon^{2/3}. \tag{4.5}$$

This gives a detailed characterization of Σ_1^ε, the range of the return map π_ε. In particular, the "diameter" of Σ_1^ε is $O(e^{-k_1/\varepsilon})$. Note that the existence of a periodic bursting solution now follows.

4.3. *Middle Branch*

Recall that the proof of the theorem depends on analyzing the two subsets Σ_1^ε and Σ_2^ε of Σ. The results we need concerning Σ_1^ε were discussed in the previous section, so we now concentrate on Σ_2^ε. These are the points in Σ which lie close to the center-stable manifold of the middle branch and therefore deviate from the behavior described in Subsection 2.2. In order to characterize this set, we begin, in this section, by analyzing the flow near the homoclinic point on the middle branch. We determine those points which must remain close to the middle branch for a finite distance before they either spiral back up or jump down to the silent phase. In later sections, we follow this set backwards by the flow until it crosses Σ; this intersection will then be Σ_2^ε.

We analyze the flow near the homoclinic orbit by choosing local coordinates near the homoclinic point. To simplify the analysis and notation, we assume that the homoclinic point is at the origin and the system is linear near the homoclinic point. We suppose this system is given by

$$\begin{aligned} x' &= \lambda_x x \\ z' &= -\lambda_z z \\ y' &= -\lambda_y \varepsilon, \end{aligned} \tag{4.6}$$

where λ_x, λ_z, and λ_y are positive constants. We assume that $\lambda_z > \lambda_x$. This actually follows from our assumption that the homoclinic orbit of (FS) bifurcates into stable periodic solutions [15].

We next define the following rectangular neighborhood of the homoclinic point as shown in Fig. 8,

$$\mathscr{B}_h = \{(x, z, y): |x| \leqslant \delta_x, |z| \leqslant \delta_z, |y| \leqslant \delta_y\}.$$

Here, δ_x, δ_z, and δ_y are small positive constants which do not depend on ε. Later, we will choose δ_y more carefully but for now it is just assumed to be sufficiently small.

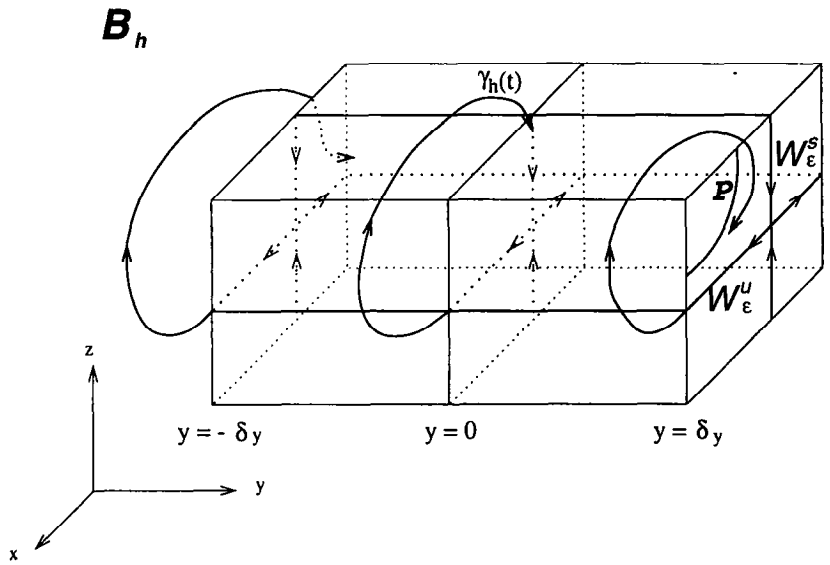

FIG. 8. The box $\mathscr{B}_h$ at the homoclinic point. The homoclinic orbit $\gamma_h(t)$ enters $\mathscr{B}_h$ through Σ_T and exists $\mathscr{B}_h$ through Σ_F.

We define the top Σ_T, front Σ_F, rear Σ_R, and left Σ_L sides of $\mathscr{B}_h$ by

$$\Sigma_T = \{(x, z, y) \in \mathscr{B}_h : z = \delta_z\}, \qquad \Sigma_F = \{(x, z, y) \in \mathscr{B}_h : x = \delta_x\}$$

$$\Sigma_R = \{(x, z, y) \in \mathscr{B}_h : x = -\delta_x\}, \qquad \Sigma_L = \{(x, z, y) \in \mathscr{B}_h : y = -\delta_y\}.$$

Assume that the homoclinic orbit $\gamma_h(t)$ enters $\mathscr{B}_h$ through Σ_T and exits $\mathscr{B}_h$ through Σ_F.

Note that every solution which begins on the top side of $\mathscr{B}_h$ must immediately enter $\mathscr{B}_h$ and then exit $\mathscr{B}_h$ through either Σ_F, Σ_R or Σ_L. If the solution leaves through Σ_F then it will give rise to another spike and if it leaves through Σ_R then it will jump down to the silent phase. We are interested in determining those points on Σ_T whose solutions leave $\mathscr{B}_h$ through Σ_L. These are the solutions which remain near the middle branch for a finite distance. Denote this subset of Σ_T by $\mathscr{L}_h$. It is a simple matter to characterize this set because we can solve the linear system (4.6) explicitly.

If $(x_0, \delta_z, y_0) \in \Sigma_T$, then the solution of (4.6) which begins at this point is

$$(x(t), z(t), y(t)) = (x_0 e^{\lambda_x t}, \delta_z e^{-\lambda_z t}, y_0 \mp \lambda_y \varepsilon t). \tag{4.7}$$

A straightforward calculation shows that a necessary condition for this solution to leave through the left side is that $|x_0| < \delta_x e^{-(1/\varepsilon)(\lambda_x/\lambda_y)(y_0+\delta_y)}$. We therefore let

$$\mathscr{L}_h = \{(x, z, y) \in \Sigma_T : |x| < \delta_x e^{-(1/\varepsilon)(\lambda_x/\lambda_y)(y+\delta_y)}\}. \tag{4.8}$$

Let $k_2 = \lambda_x \delta_y / \lambda_y$. Then the "width" of $\mathscr{L}_h$ is of $O(e^{-k_2/\varepsilon})$ near the homoclinic point.

We now choose δ_y more carefully. In order to prove the uniqueness result, we will need that the expansion of trajectories which begin in $\Sigma_T \backslash \mathscr{L}_h$ is less than the compression which must take place along the lower branch. It is straightforward to estimate this expansion since while in $\mathscr{B}_h$, the trajectories are given by (4.7). If $(x, \delta_z, y) \in \Sigma \backslash \mathscr{L}_h$ and $y < 0$, then $|x| > \delta_x e^{-k_2/\varepsilon}$. It follows that the maximum possible expansion passing near the homoclinic point is $O(e^{k_2/\varepsilon})$. We choose δ_y so small that $k_2 < k_1$ where k_1 is as in (4.4). The possible expansion of trajectories in $\mathscr{B}_h$ is now dominated by the compression along the lower branch.

The formal definition of Σ_2^ε is those points in Σ whose trajectories cross $\mathscr{L}_h$ before returning to Σ. Note that $\mathscr{L}_h$ is a very thin neighborhood of W_ε^s near the homoclinic point. We analyze Σ_2^ε by following W_ε^s backwards until it crosses Σ. This is done in the next two sections.

4.4. *Periodic Branch*

We now consider the nature of the flow near $\mathscr{P}$ for $\varepsilon > 0$. For this analysis, we must restrict ourselves to a region bounded away from the homoclinic orbit. We therefore consider a neighborhood of $\mathscr{P}$ for which $y > \delta_y$ where δ_y was defined in the preceding section.

We assume that the manifold $\mathscr{P}$ is normally hyperbolic. This then implies that $\mathscr{P}$ perturbs to a manifold, which we denote by $\mathscr{P}_\varepsilon$, that is invariant with respect to (2.1) for ε sufficiently small [10]. The "distance" between $\mathscr{P}$ to $\mathscr{P}_\varepsilon$ is $O(\varepsilon)$. Since $\mathscr{P}$ is assumed to be attracting, it follows that $\mathscr{P}_\varepsilon$ is also attracting.

It is now necessary to analyze the flow on the invariant manifold $\mathscr{P}_\varepsilon$ and the asymptotic behavior of trajectories which lie close to $\mathscr{P}_\varepsilon$. Since $y' < 0$ near $\mathscr{P}_\varepsilon$ and $\mathscr{P}_\varepsilon$ is topologically a cylinder, it is clear that trajectories spiral around $\mathscr{P}_\varepsilon$ moving to the "left" at a rate which is $O(\varepsilon)$. In order to obtain detailed estimates concerning this flow, it will be convenient to consider the natural return map defined by the flow. Let Σ_P be a two-dimensional section which is transverse to $\mathscr{P}$ as shown in Fig. 9. Note that Σ_P intersects $\mathscr{P}_\varepsilon$ along a one-dimensional curve which we denote by L_ε. We may parameterize L_ε by y for $\delta_y < y < y_0$. Here, $y_0 = y_\rho + \delta_\rho$ where δ_ρ is a small positive constant. Then the flow gives rise to a map from some subset of L_ε into L_ε. Projecting onto the y-axis, this induces a map $H_\varepsilon(y)$ from some

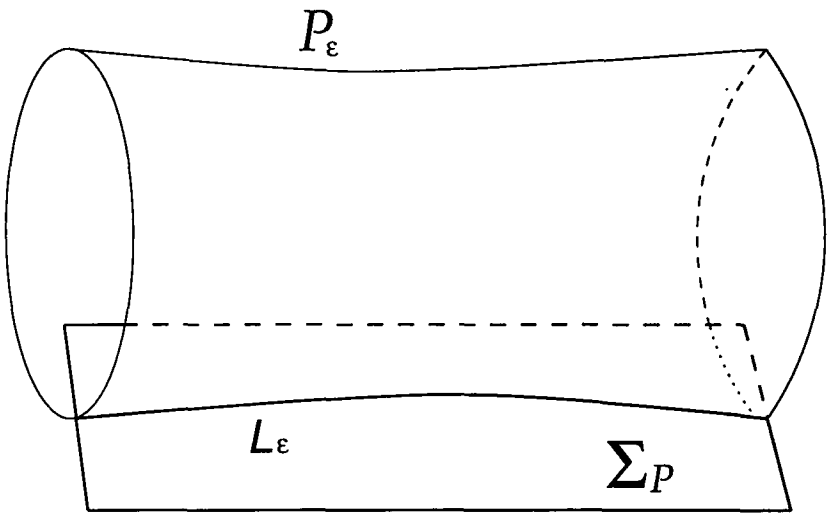

FIG. 9. The two-dimensional section Σ_P which is transverse to $\mathscr{P}$. The section Σ_P intersects $\mathscr{P}_\varepsilon$ along the curve L_ε.

subset of the interval (δ_y, y_0) back into this interval. Note that we can choose the domain of this map to be as close to (δ_y, y_0) as we please by choosing ε sufficiently small.

Now when $\varepsilon = 0$, we have that $H_0(y) = y$. It follows that we can write $H_\varepsilon(y) = y + \varepsilon h(y, \varepsilon)$ where h is $O(1)$ with respect to ε. The following lemma gives the nature of h for ε very small. The proof of this lemma is straightforward; see, for example, [15].

LEMMA 4.1. *For each* $y \in [\delta_y, y_0]$, *let* $p_y(t) = X^*(t, y)$ *be the periodic orbit of* (*FS*) *and let* $T(y)$ *be its period. Then*

$$\lim_{\varepsilon \to 0} h(y, \varepsilon) = \int_0^{T(y)} g(X^*(t, y), y)\, dt = T(y)\, \bar{g}(y),$$

where $\bar{g}(y)$ *is the average value of* g *on the periodic orbit* $X^*(t, y)$.

It is clear from Lemma 4.1 that $h(y, 0) = \lim_{\varepsilon \to 0} h(y, \varepsilon) < -K$ uniformly in $[\delta_y, y_0]$ with some constant $K > 0$. A useful consequence of this lemma is that it allows us to estimate the rate of expansion of nearby trajectories on $\mathscr{P}_\varepsilon$. That is, choose y_1 and y_2 in the domain of H_ε. By Lemma 4.1, there exists a Lipschitz constant m such that

$$|h(y_1, \varepsilon) - h(y_2, \varepsilon)| \leqslant m\, |y_1 - y_2|$$

holds for all sufficiently small $\varepsilon > 0$. Therefore,

$$|H_\varepsilon(y_1) - H_\varepsilon(y_2)| \leqslant (1 + m\varepsilon)\,|y_1 - y_2|.$$

Repeating this step n times,

$$|H_\varepsilon^n(y_1) - H_\varepsilon^n(y_2)| \leqslant (1 + m\varepsilon)^n\,|y_1 - y_2|.$$

Note that there must exist a constant c which does not depend on n or ε such that if $H_\varepsilon^n(y_1)$ and $H_\varepsilon^n(y_2)$ are in the domain of H_ε after n iterations, then $n < c/\varepsilon$. Hence,

$$|H_\varepsilon^n(y_1) - H_\varepsilon^n(y_2)| \leqslant (1 + m\varepsilon)^{c/\varepsilon}\,|y_1 - y_2|.$$

As $\varepsilon \to 0$, the term $(1 + m\varepsilon)^{c/\varepsilon}$ converges to the constant $M = e^{mc}$. We conclude that

$$|H_\varepsilon^n(y_1) - H_\varepsilon^n(y_2)| \leqslant M\,|y_1 - y_2|.$$

Note that the constant M is independent of ε.

By reversing time, we obtain a similar estimate. We have therefore proven the following result which gives a bound on the possible expansion of trajectories near $\mathscr{P}_\varepsilon$.

PROPOSITION 4.2. *There exist positive constants M_1 and M_2 such that if y_1, y_2, $H_\varepsilon^n(y_1)$ and $H_\varepsilon^n(y_2)$ all lie in the domain of H_ε, then*

$$M_1\,|y_1 - y_2| \leqslant |H_\varepsilon^n(y_1) - H_\varepsilon^n(y_2)| \leqslant M_2\,|y_1 - y_2|.$$

We conclude this section by discussing properties of solutions which lie close to $\mathscr{P}_\varepsilon$. For this, we use results from the geometric theory of singular perturbations developed by Fenichel [13]. We begin by discussing the notion of *asymptotic phase*. Let q be any point sufficiently close to $\mathscr{P}_\varepsilon$ and let $q(t)$ be the solution of (2.1) with $q(0) = q$. Since $\mathscr{P}_\varepsilon$ is attracting, it follows that $q(t)$ approaches $\mathscr{P}_\varepsilon$ at an exponential rate (at least until it reaches the left boundary of $\mathscr{P}_\varepsilon$ near $y = \delta_y$). The results of Fenichel imply that much more is true: $q(t)$ actually approaches a specific orbit $p(t)$ which lies on the invariant manifold $\mathscr{P}_\varepsilon$. That is, there is an orbit $p(t)$ with $p(0) = p \in \mathscr{P}_\varepsilon$ such that

$$|p(t) - q(t)| \leqslant Ce^{-\kappa t/\varepsilon} \tag{4.9}$$

for constants C and κ which do not depend on ε or the points p and q. This estimate remains valid as long as the trajectories remain near $\mathscr{P}_\varepsilon$.

If (4.9) holds, then we say that p and q have the same asymptotic phase. For each $p \in \mathscr{P}_\varepsilon$, let $\mathscr{F}_\varepsilon(p)$ be the set of points which have the same

asymptotic phase as p. Fenichel's theory provides the following characterization of this set.

First suppose that $\varepsilon = 0$ and $p = (v_0, w_0, y_0) \in \mathscr{P}$. Then $p(t)$ is a periodic orbit which is asymptotically stable with respect to the fast system. Standard perturbation theory implies that $\mathscr{F}_0(p)$ is a one-dimensional curve which intersects the manifold $\mathscr{P}$ transversely and lies in the plane $y = y_0$. Hence, $\bigcup_{t>0} \mathscr{F}_0(p(t))$ is a two-dimensional "punctured sheet" that lies in the plane $y = y_0$.

If $\varepsilon > 0$ is sufficiently small and $p = (v_0, w_0, y_0) \in \mathscr{P}_\varepsilon$, then the fiber $\mathscr{F}_\varepsilon(p)$ is still a smooth one-dimensional curve which lies C^1 close to the plane $y = y_0$. Moreover, $p(t) \in \mathscr{P}_\varepsilon$ for $0 < t < T$ where $T = O(1/\varepsilon)$. Then $\mathscr{F}_\varepsilon^*(p) \equiv \bigcup_{0<t<T} \mathscr{F}_\varepsilon(p(t))$ is the set of all points which asymptotically approach the entire trajectory $p(t)$. Since $p(t)$ resembles a helix and each $\mathscr{F}_\varepsilon(p(t))$ is a one-dimensional fiber, it follows that $\mathscr{F}_\varepsilon^*(p)$ is a two-dimensional, cork-screw-shaped object as shown in Fig. 10.

4.5. *Homoclinic Orbit*

The goal of this section is to understand how $\mathscr{P}_\varepsilon$ intersects $\mathscr{L}_h \subset \Sigma_T$. The key step in this analysis is to show that the curves $W_\varepsilon^s \cap \Sigma_T$ and $\mathscr{P}_\varepsilon \cap \Sigma_T$ intersect transversely. The main difficulty is that Fenichel's results imply

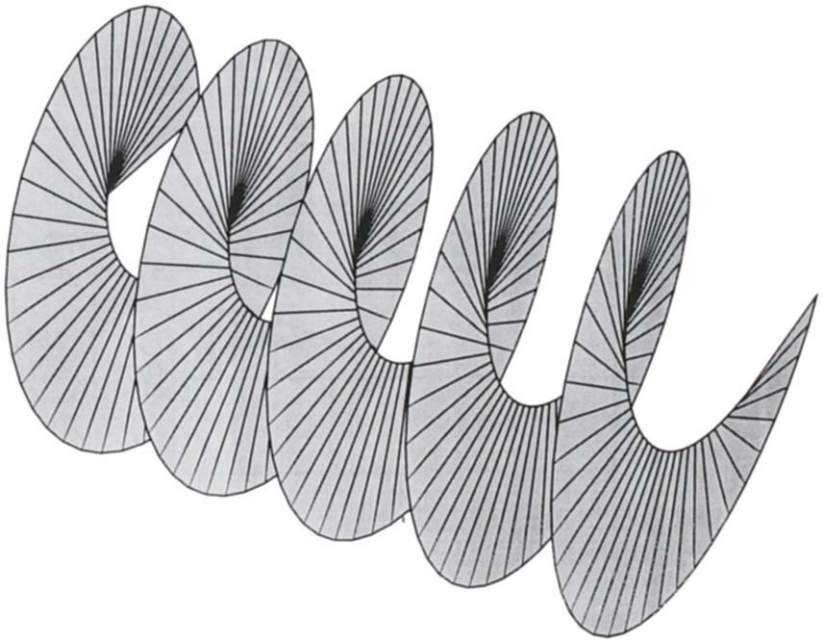

FIG. 10. The set $\mathscr{F}_\varepsilon^*(p)$ is a two-dimensional, cork-screw-shaped object.

that $\mathscr{P}_\varepsilon$ is well defined only for some finite distance bounded away from the homoclinic orbit of (FS). Therefore, we need to analyze, in more detail, the dynamics near the homoclinic orbit. For this, we consider a map $\pi(\varepsilon)$ defined by the flow from a subset of Σ_T to Σ_T. This map is the composition of two other maps; that is, $\pi(\varepsilon) = \psi(\varepsilon) \circ \phi(\varepsilon)$. The properties needed for each of these maps are described below.

(i) *Flow-Defined Map* $\phi(\varepsilon)$. Trajectories which begin on $\Sigma_T^+ \equiv \{(x, z, y) \in \Sigma_T : x > 0\}$ exit $\mathscr{B}_h$ through either Σ_F or Σ_L. Let $Dom(\phi)$ be all the points of Σ_T^+ whose trajectories exit through Σ_F and let $\phi(\varepsilon) : Dom(\phi) \subset \Sigma_T^+ \to \Sigma_F$ be the corresponding flow-defined map. See Fig. 11. Note that $Dom(\phi)$ depends on ε and $Dom(\phi) \to \Sigma_T^+$ as $\varepsilon \to 0$.

From (4.6), we can compute an explicit formula for $\phi(\varepsilon)$. If $(x, \delta_z, y) \in Dom(\phi)$, then

$$\phi(\varepsilon)(x, \delta_z, y) = (\delta_x, \phi_z(x, y), \phi_y(x, y))$$

where

$$\begin{cases} \phi_z(x, y) = \delta_z (x/\delta_x)^{\lambda_z/\lambda_x} \\ \phi_y(x, y) = y - \varepsilon \dfrac{\lambda_y}{\lambda_x} \ln(\delta_x/x). \end{cases} \tag{4.10}$$

The following lemma is an immediate consequence of this explicit formula.

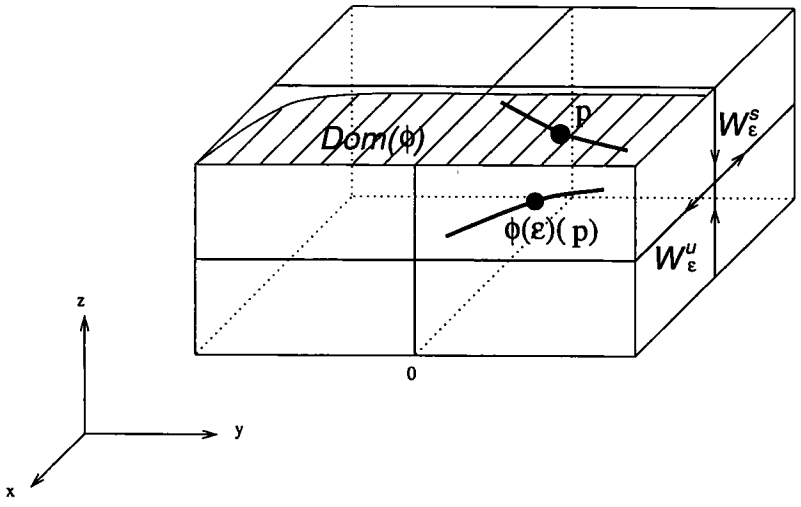

FIG. 11. Flow-defined map $\phi(\varepsilon)$. This map is defined by the solutions of (4.6) near the homoclinic point.

LEMMA 4.3. *Assume that $\alpha(y)$ is a smooth, increasing function such that the curve*

$$\tilde{\alpha} = \{(x, \delta_z, y) \in \Sigma_T^+ : x = \alpha(y)\} \subset Dom(\phi).$$

Then $\phi(\varepsilon)(\tilde{\alpha})$ is a smooth curve in Σ_F which can be written as $\tilde{\beta} = \{(\delta_x, z, y) \in \Sigma_F : z = \beta(y)\}$ where $\beta'(y) > 0$ for each y.

(ii) *Flow-Defined Map $\psi(\varepsilon)$.* The homoclinic orbit $\gamma_h(t)$ intersects Σ_F at $(\delta_x, 0, 0)$ and intersects Σ_T at $(0, \delta_z, 0)$. Therefore, when $\varepsilon = 0$ the flow defines a diffeomorphism from a neighborhood of $(\delta_x, 0, 0) \in \Sigma_F$ onto a neighborhood of $(0, \delta_z, 0)$ in Σ_T. We can find a fixed (independent of ε) set $Dom(\psi)$ containing $(\delta_x, 0, 0)$ in Σ_F such that the flow-defined map $\psi(\varepsilon)$: $Dom(\psi) \subset \Sigma_F \to \Sigma_T$ is a diffeomorphism from a subset of Σ_F into Σ_T for all sufficiently small ε. See Fig. 12. Suppose that $\psi(\varepsilon)(\delta_x, z, y) = (\psi_x(z, y), \delta_z, \psi_y(z, y))$ and let $\psi(\varepsilon)(z, y) = (\psi_x(z, y), \psi_y(z, y))$. Note that the functions $\psi_x(z, y)$ and $\psi_y(z, y)$ actually depend on ε.

We need to estimate $D\psi(\varepsilon)$. Since $\psi(\varepsilon)$ is a regular perturbation of $\psi(0)$, we first compute $D\psi(0)$. Note that when $\varepsilon = 0$, $\psi_y(z, y) = y$. Hence,

$$\frac{\partial \psi_y}{\partial z} = 0 \qquad \text{and} \qquad \frac{\partial \psi_y}{\partial y} = 1.$$

In order to compute $\partial \psi_x / \partial y$, let $l^u = \{(\delta_x, z, y) \in \Sigma_F : z = 0\}$. The assumption that W_0^s and W_0^u intersect transversely implies we can write

$$\psi(0)(l^u) = \{(x, \delta_z, y) \in \Sigma_T : x = h(y)\}$$

where $h(y)$ is a smooth function with $h(0) = 0$ and $h'(0) > 0$. Then $(\partial \psi_x / \partial y)(0, 0) = h'(0)$. Finally, let $b = (\partial \psi_x / \partial z)(0, 0)$. It is not difficult to see that $b > 0$. Putting this all together, we find that

$$D\hat{\psi}(0) = \begin{bmatrix} \dfrac{\partial \psi_x}{\partial z}(0, 0) & \dfrac{\partial \psi_x}{\partial y}(0, 0) \\ \dfrac{\partial \psi_y}{\partial z}(0, 0) & \dfrac{\partial \psi_y}{\partial y}(0, 0) \end{bmatrix} = \begin{bmatrix} b & h'(0) \\ 0 & 1 \end{bmatrix}.$$

Since $\psi(\varepsilon)$ is a smooth regular, perturbation of $\psi(0)$, we have the following result.

LEMMA 4.4. *Assume that $\alpha(y)$ is a smooth, increasing function such that*

$$\tilde{\alpha} = \{(\delta_x, z, y) \in \Sigma_F : z = \alpha(y)\} \subset Dom(\psi).$$

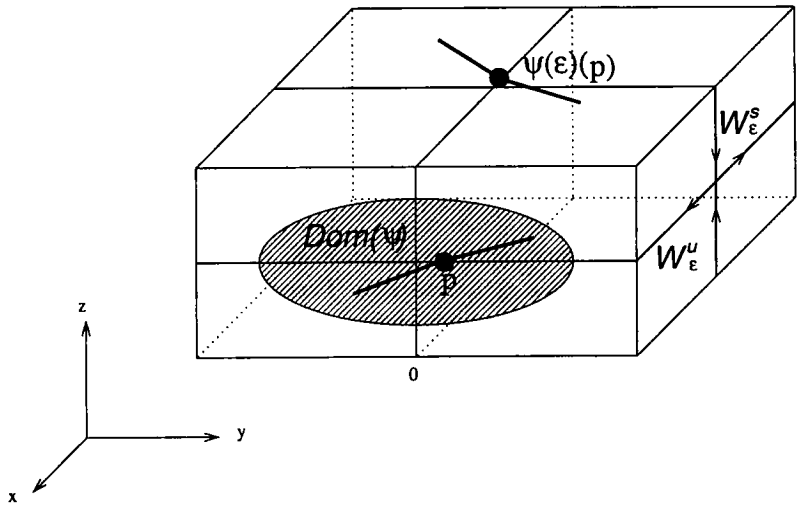

FIG. 12. Flow-defined map $\psi(\varepsilon)$. This map is a diffeomorphism from a subset of Σ_F into Σ_T.

Then $\psi(\varepsilon)(\tilde{\alpha})$ *is a smooth curve which can be written as* $\tilde{\beta} = \{(x, \delta_z, y) \in \Sigma_T : x = \beta(y)\}$ *where* $\beta'(y) > h'(0)/2$ *for each* y.

(iii) *Flow-Defined Map* $\pi(\varepsilon)$. Since $\pi(\varepsilon) = \psi(\varepsilon) \circ \phi(\varepsilon)$, the following result follows from Lemmas 4.3 and 4.4.

PROPOSITION 4.5. *Assume that* $\alpha(y)$ *is a smooth, increasing function such that*

$$\tilde{\alpha} = \{(x, \delta_z, y) \in \Sigma_T^+ : x = \alpha(y)\} \subset Dom(\pi)$$

Then $\pi(\varepsilon)(\tilde{\alpha})$ *can be written as* $\tilde{\beta} = \{(x, \delta_z, y) \in \Sigma_T : x = \beta(y)\}$ *where* $\beta'(y) > h'(0)/2$ *for each* y.

Now consider $\mathscr{P}_\varepsilon \cap \Sigma_T$. Fenichel's results guarantee that this is a well defined, smooth curve for $y > \delta_y$. Using Proposition 4.5 we can extend this curve for values of $y < \delta_y$ by considering the iterates $\pi^k(\varepsilon)(\mathscr{P}_\varepsilon \cap \Sigma_T)$ for $k \geqslant 1$. Since $\mathscr{P}_\varepsilon$ is invariant and $y' < 0$ along $\mathscr{P}_\varepsilon$, it follows that after each iterate, $\mathscr{P}_\varepsilon \cap \Sigma_T$ is extended to the left by a distance $O(\varepsilon)$. Moreover, if this curve is given by $\zeta_\varepsilon = \{(x, \delta_z, y) \in \Sigma_T : x = h_\varepsilon(y)\}$, then $h_\varepsilon'(y) > h'(0)/2$. Hence, ζ_ε must intersect $W^s_\varepsilon \cap \Sigma_T$ transversely. This is shown in Fig. 13.

We now consider $\mathscr{P}_\varepsilon \cap \mathscr{L}_h$. From (4.8), $\mathscr{L}_h$ is a thin strip containing W^s_ε whose "width" is $O(e^{-k_2/\varepsilon})$. Since ζ_ε intersects $W^s_\varepsilon \cap \Sigma_T$ transversely, it follows that

$$\mathscr{C}_\varepsilon \equiv \mathscr{P}_\varepsilon \cap \mathscr{L}_h = \zeta_\varepsilon \cap \mathscr{L}_h$$

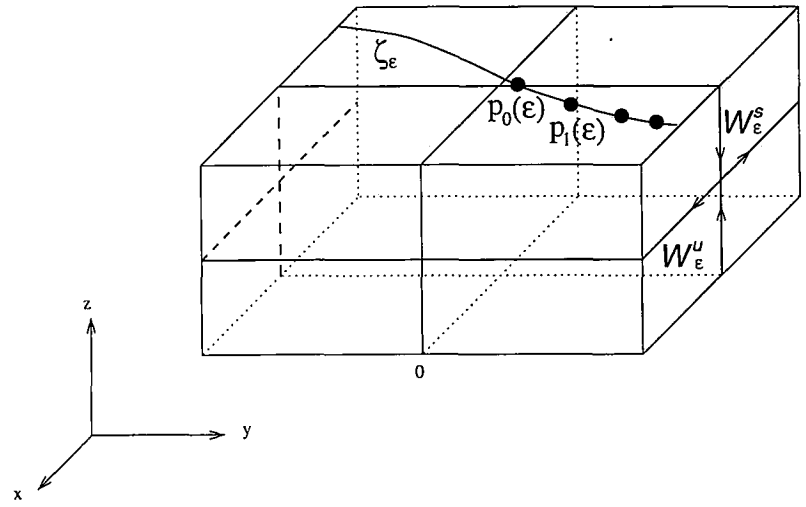

FIG. 13. The curve ζ_ε. This curve is extended from $\mathscr{P}_\varepsilon \cap \Sigma_T$ by the iterates $\pi^k(\varepsilon)(\mathscr{P}_\varepsilon \cap \Sigma_T)$ for $k \geqslant 1$. The point $p_0(\varepsilon)$ is the intersection of $\mathscr{P}_\varepsilon$ and W^s_ε on Σ_T.

is curve of length $O(e^{-k_2/\varepsilon})$. If we now follow the trajectories through $\mathscr{C}_\varepsilon$ backwards in time, they will form what resembles a spiraling strip wrapped around $\mathscr{P}_\varepsilon$. We denote this strip by $\mathscr{S}_\varepsilon$. According to Proposition 4.2, the width of $\mathscr{S}_\varepsilon$ remains $O(e^{-k_2/\varepsilon})$.

4.6. *The set* Σ_2^ε

We are now able to characterize the set Σ_2^ε. Recall that this was defined as those points in Σ which lie "close" to W^s_ε, the center-stable manifold of the middle branch. More precisely, Σ_2^ε are those points in Σ whose trajectories cross $\mathscr{L}_h$. Hence, we need to follow the trajectories through $\mathscr{L}_h$ backwards until they cross Σ. This is done by noting that each point in Σ has the same asymptotic phase as a point on $\mathscr{P}_\varepsilon$. If $q \in \Sigma_2^\varepsilon$ has the same asymptotic phase as $p \in \mathscr{P}_\varepsilon$, then, using (4.9), the distance between the points where the trajectories starting at q and p cross $\mathscr{L}_h$ is $O(e^{-\kappa/\varepsilon})$. Hence in order to characterize Σ_2^ε it suffices to first consider $\mathscr{L}_h \cap \mathscr{P}_\varepsilon$. We follow this set backwards in time as it spirals around $\mathscr{P}_\varepsilon$. Then Σ_2^ε consists of those points where the fibers of this spiraling set cross Σ. Now this spiraling set is precisely $\mathscr{S}_\varepsilon$, defined in the previous section. The width of this set is $O(e^{-k_2/\varepsilon})$ and Fenichel's results imply that the "width" of the fibers emanating from $\mathscr{S}_\varepsilon$ remain $O(e^{-k_2/\varepsilon})$. Hence, this cork-screw set of fibers must intersect Σ along strips whose "width" are $O(e^{-k_2/\varepsilon})$. Finally, we note that the rate at which the fibers spiral around is determined by the slow equation; that is the rate is $O(\varepsilon)$. Hence, the distance between the strips on Σ must be $O(\varepsilon)$. This is illustrated in Fig. 6.

5. COMPLETION OF THE PROOF

It will be convenient to introduce the following notation. We say that $g(\varepsilon)$ is asymptotically $O(f(\varepsilon))$ and write $g(\varepsilon) \asymp O(f(\varepsilon))$ if there exist positive constants c_1 and c_2 such that $c_1 f(\varepsilon) \leqslant g(\varepsilon) \leqslant c_2 f(\varepsilon)$ for all $\varepsilon > 0$ sufficiently small.

5.1. *Uniqueness If* $\Sigma_1^\varepsilon \cap \Sigma_2^\varepsilon = \varnothing$

The analysis in the proceeding section demonstrates that the bursting solution is uniquely determined for those values of ε for which $\Sigma_1^\varepsilon \cap \Sigma_2^\varepsilon = \varnothing$. This is because the contraction that must take place along the lower branch will dominate any possible expansion that can arise other places. The contraction along the lower branch and past the right knee is $O(e^{-k_1/\varepsilon})$, while any expansion near $\mathscr{P}_\varepsilon$ is at most linear and the expansion near the middle branch is at most $O(e^{k_2/\varepsilon})$ where $k_2 < k_1$. Note that any possible expansion during either the jumping up or jumping down processes are at most $O(1)$ with respect to ε.

5.2. *When Is* $\Sigma_1^\varepsilon \cap \Sigma_2^\varepsilon \neq \varnothing$?

In order to complete the proof of Theorem 3.1, we must characterize those values of ε for which $\Sigma_1^\varepsilon \cap \Sigma_2^\varepsilon \neq \varnothing$. Recall that Σ_1^ε is a very small set, of diameter $O(e^{-k_1/\varepsilon})$, which lies very close to the point $\bar{P}_\varepsilon^1$. Moreover, Σ_2^ε consists of a large number of narrow strips of width of $O(e^{-k_2/\varepsilon})$. The distance between adjacent strips is $O(\varepsilon)$. We estimate the values of ε for which these sets can intersect by determining how the sets change their positions as ε is varied. According to (4.3) and (4.5), Σ_1^ε approaches the point P_0 as $\varepsilon \to 0$; the rate at which the y-components of the points in Σ_1^ε approach y_ρ is asymptotically $O(\varepsilon^{-1/3})$. We prove below that the rate at which the y-components of each strip in Σ_2^ε change with respect to ε is asymptotically $O(\varepsilon^{-1})$. Since Σ_1^ε and Σ_2^ε move at different rates, it follows that each strip in Σ_2^ε must pass through the set Σ_1^ε as ε decreases to 0. More precisely, this will complete the proof of Theorem 3.1 for the following reason. In what follows, $c_0, c_1, \ldots$ and $C_0, C_1, \ldots$ are positive constants which do not depend on ε.

Suppose that ε_0 is such that $\bar{P}_{\varepsilon_0}^1$ lies on the left boundary of one of the strips in Σ_2^ε. Let $\varepsilon_0^* < \varepsilon_0$ be the value of ε when $\bar{P}_{\varepsilon_0^*}^1$ crosses the right boundary of this strip. Then, for $\varepsilon_0^* \leqslant \varepsilon \leqslant \varepsilon_0$, the maximum y-direction velocity of $\bar{P}_\varepsilon^1$ is less than $c_0/(\varepsilon_0^*)^{1/3}$ and the minimum y-direction velocity of the given strip is greater than c_1/ε_0. Since the width of the strip is $O(e^{-k_2/\varepsilon_0})$, it follows that

$$\varepsilon_0 - \varepsilon_0^* \leqslant \frac{c_2 e^{-k_2/\varepsilon_0}}{c_1 \varepsilon_0^{-1} - c_0(\varepsilon_0^*)^{-1/3}}.$$

Since $\varepsilon_0^* > \varepsilon_0/2$, it follows that $\varepsilon_0 - \varepsilon_0^* = O(e^{-k_2/\varepsilon_0})$. As ε decreases to 0, $\bar{P}_\varepsilon^1$ crosses the region between the strips and reaches the left boundary of the next strip for some $\varepsilon = \varepsilon_1$. The distance between adjacent strips is greater than $c_3\varepsilon_1$. Therefore,

$$\varepsilon_0 - \varepsilon_1 \geqslant \frac{c_3\varepsilon_1}{c_4\varepsilon_1^{-1} - c_5\varepsilon_0^{-1/3}} = \frac{(c_3/c_5)\,\varepsilon_1^2}{c_4/c_5 - \varepsilon_1/\varepsilon_0^{1/3}}. \tag{5.1}$$

Since $\varepsilon_1 < \varepsilon_0$, it follows that $0 < \varepsilon_1/\varepsilon_0^{1/3} \leqslant \varepsilon_0^{2/3} \ll 1$. Hence, $0 < c_4/c_5 - \varepsilon_1/\varepsilon_0^{1/3} \leqslant c_4/c_5$ and, from (5.1),

$$\varepsilon_0 - \varepsilon_1 \geqslant \frac{(c_3/c_5)\,\varepsilon_1^2}{c_4/c_5}.$$

In particular, $\varepsilon_1 > \varepsilon_0/2$, from which it follows that $\varepsilon_0 - \varepsilon_1 \geqslant C_0\varepsilon_0^2$ for some C_0. In this way, we construct a sequence $\{\varepsilon_i\} \to 0$ with $\varepsilon_i - \varepsilon_{i+1} \geqslant C_0\varepsilon_i^2$. Note that C_0 is independent of i. If $k < k_2 < k_1$, then $\Sigma_1^\varepsilon \cap \Sigma_2^\varepsilon = \varnothing$ if ε is not in an $O(e^{-k/\varepsilon_i})$ neighborhood of ε_i for each $i = 0, 1, \ldots$. This completes the proof of our main theorem.

It remains to demonstrate that the rate at which the y-components of each strip in Σ_2^ε changes with respect to ε is asymptotically $O(\varepsilon^{-1})$. This is done in the next section.

5.3. *How Do the Strips in Σ_2^ε Change with Respect to ε?*

Recall that $\mathscr{P}_\varepsilon$ and W_ε^s intersect transversely at a point $p_0(\varepsilon)$ on Σ_T. Let $p_n(\varepsilon) = \pi^{-n}(\varepsilon)(p_0(\varepsilon))$ for $1 \leqslant n \leqslant N_0$ where N_0 is chosen so that $p_n(\varepsilon)$ remains in $\mathscr{B}_h$ for $1 \leqslant n \leqslant N_0$. See Fig. 13. We define $p_n(\varepsilon)$ for $n > N_0$ using the return map for the section Σ_P to $\mathscr{P}_\varepsilon$ defined in Section 4.4. Let $p_n(\varepsilon) = (x_n(\varepsilon), \delta_z, y_n(\varepsilon))$. Choose N so that $|y_N(\varepsilon) - y_\rho| < \delta_\rho$; recall that y_ρ is the y-component of the right knee and δ_ρ is a small positive constant. We will prove that there exist positive constants c^1 and c^2 such that

$$\frac{c^1}{\varepsilon} < \frac{d}{d\varepsilon}\, y_N(\varepsilon) < \frac{c^2}{\varepsilon}. \tag{5.2}$$

Using our previous analysis, this will then imply that the rate at which each strip in Σ_2^ε changes with respect to ε is asymptotically $O(\varepsilon^{-1})$.

To prove (5.2) we consider the cases $n < N_0$ and $n \geqslant N_0$ separately. We now assume that $n < N_0$. Then $p_n(\varepsilon) \in \mathscr{B}_h$ and we can estimate $y_n(\varepsilon) - y_{n-1}(\varepsilon)$ by considering the composition of the two maps $\psi^{-1}(\varepsilon)$ and $\phi^{-1}(\varepsilon)$. Note that each $p_n(\varepsilon)$ must lie on the curve ξ_ε defined in Section 4.5.

Hence, $x_n(\varepsilon) = h_\varepsilon(y_n(\varepsilon))$. Let $\hat{y}_n(\varepsilon)$ be the y-component of $\psi^{-1}(\varepsilon)(p_n(\varepsilon))$. It is easy to see that there exists a smooth function $k(y, \varepsilon)$ which is $O(1)$ with respect to ε such that $\hat{y}_n(\varepsilon) = y_n(\varepsilon) + \varepsilon k(y_n(\varepsilon), \varepsilon)$. Moreover, there exists $K > 0$ such that $\lim_{\varepsilon \to 0} k(y, \varepsilon) = k(y, 0) > K$ uniformly on $[-\delta_y, \delta_y]$. Now $p_n(\varepsilon) = \pi^{-1}(\varepsilon)(p_{n-1}(\varepsilon))$. Using (4.10), this implies that

$$\hat{y}_{n-1}(\varepsilon) = y_n(\varepsilon) - \varepsilon \frac{\lambda_y}{\lambda_x} \ln\left(\frac{\delta_x}{x_n(\varepsilon)}\right)$$

or

$$y_n(\varepsilon) - y_{n-1}(\varepsilon) = \varepsilon k(y_{n-1}(\varepsilon), \varepsilon) + \varepsilon \frac{\lambda_y}{\lambda_x} \ln\left(\frac{\delta_x}{x_n(\varepsilon)}\right), \tag{5.3}$$

where $x_n(\varepsilon) = h_\varepsilon(y_n(\varepsilon))$. It is clear that $y_n(\varepsilon) - y_{n-1}(\varepsilon) \geqslant c_1 \varepsilon$ for some constant c_1 which does not depend on n as long as $y_n(\varepsilon) < y_h + \delta_y$. Therefore, $y_n(\varepsilon) - y_0(\varepsilon) \geqslant n c_1 \varepsilon$ and so $x_n(\varepsilon) \geqslant n c_2 \varepsilon$ for some other constant $c_2 > 0$.

Let $\xi_\varepsilon(y) \equiv h_\varepsilon(y + y_0(\varepsilon))$. It follows from (5.3) with $n = 1$ that

$$\xi_\varepsilon^{-1}(x_1(\varepsilon)) = \varepsilon k(y_0(\varepsilon), \varepsilon) + \varepsilon \frac{\lambda_y}{\lambda_x} \ln\left(\frac{\delta_x}{x_1(\varepsilon)}\right).$$

Differentiating with respect to ε,

$$\frac{\partial \xi_\varepsilon^{-1}}{\partial x} \cdot x_1'(\varepsilon) = k + \varepsilon \left\{\frac{\partial k}{\partial y} \cdot y_0'(\varepsilon) + \frac{\partial k}{\partial \varepsilon}\right\} + \frac{\lambda_y}{\lambda_x} \left\{\ln\left(\frac{\delta_x}{x_1(\varepsilon)}\right) - \varepsilon \frac{x_1'(\varepsilon)}{x_1(\varepsilon)}\right\} - \frac{\partial \xi_\varepsilon^{-1}}{\partial \varepsilon}.$$

Here $'$ denotes the derivative with respect to ε and $k = k(y_0(\varepsilon), \varepsilon)$ and $\xi_\varepsilon^{-1} = \xi_\varepsilon^{-1}(x_1(\varepsilon))$. Solving for $x_1'(\varepsilon)$,

$$x_1'(\varepsilon) \left\{\frac{\partial \xi_\varepsilon^{-1}}{\partial x} + \varepsilon \frac{\lambda_y}{\lambda_x} \frac{1}{x_1(\varepsilon)}\right\} = k + \varepsilon \left\{\frac{\partial k}{\partial y} \cdot y_0'(\varepsilon) + \frac{\partial k}{\partial \varepsilon}\right\} + \frac{\lambda_y}{\lambda_x} \ln\left(\frac{\delta_x}{x_1(\varepsilon)}\right) - \frac{\partial \xi_\varepsilon^{-1}}{\partial \varepsilon}.$$

Since the right hand side term is positive and $\partial \xi_\varepsilon^{-1} / \partial x > 0$, we conclude $x_1'(\varepsilon) > 0$. We now use induction on n to show that $x_n'(\varepsilon) > 0$. By (5.3),

$$x_n'(\varepsilon)\left\{\frac{\partial \xi_\varepsilon^{-1}}{\partial x}(x_n(\varepsilon))+\varepsilon\frac{\lambda_y}{\lambda_x}\frac{1}{x_n(\varepsilon)}\right\}=x_{n-1}'(\varepsilon)\cdot\frac{\partial \xi_\varepsilon^{-1}}{\partial x}(x_{n-1}(\varepsilon))+k$$
$$+\varepsilon\left\{\frac{\partial k}{\partial y}\cdot y_{n-1}'(\varepsilon)+\frac{\partial k}{\partial \varepsilon}\right\}+\frac{\lambda_y}{\lambda_x}\ln\left(\frac{\delta_x}{x_n(\varepsilon)}\right)$$
$$+\frac{\partial \xi_\varepsilon^{-1}}{\partial \varepsilon}(x_{n-1}(\varepsilon))-\frac{\partial \xi_\varepsilon^{-1}}{\partial \varepsilon}(x_n(\varepsilon)),$$

where $k=k(y_{n-1}(\varepsilon),\varepsilon)$. Assuming $x_{n-1}'(\varepsilon)>0$, it follows that $x_n'(\varepsilon)>0$.

Suppose $\varepsilon=\varepsilon^*>0$ and $\Delta\varepsilon$ is a small increment of ε. Let $\varepsilon^{**}=\varepsilon^*+\Delta\varepsilon$. Then,

$$y_n(\varepsilon^{**})-y_n(\varepsilon^*)=y_{n-1}(\varepsilon^{**})-y_{n-1}(\varepsilon^*)$$
$$+\varepsilon^{**}k(y_{n-1}(\varepsilon^{**}),\varepsilon^{**})-\varepsilon^*k(y_{n-1}(\varepsilon^*),\varepsilon^*)$$
$$+\frac{\lambda_y}{\lambda_x}\varepsilon^{**}\ln\left(\frac{\delta_x}{x_n(\varepsilon^{**})}\right)-\frac{\lambda_y}{\lambda_x}\varepsilon^*\ln\left(\frac{\delta_x}{x_n(\varepsilon^*)}\right).$$

Now

$$\varepsilon^{**}k(y_{n-1}(\varepsilon^{**}),\varepsilon^{**})-\varepsilon^*k(y_{n-1}(\varepsilon^*),\varepsilon^*)$$
$$=\Delta\varepsilon k(y_{n-1}(\varepsilon^{**}),\varepsilon^{**})+\varepsilon^*\{k(y_{n-1}(\varepsilon^{**}),\varepsilon^{**})-k(y_{n-1}(\varepsilon^{**}),\varepsilon^*)\}$$
$$+\varepsilon^*\{k(y_{n-1}(\varepsilon^{**}),\varepsilon^*)-k(y_{n-1}(\varepsilon^*),\varepsilon^*)\}$$
$$\leqslant\Delta\varepsilon(K_1+K_2\varepsilon^*)+K_3\varepsilon^*\{y_{n-1}(\varepsilon^{**})-y_{n-1}(\varepsilon^*)\}$$

where $K_1>0$, K_2 and $K_3\geqslant 0$ are constants which can be chosen independent of ε. Moreover,

$$\frac{\lambda_y}{\lambda_x}\varepsilon^{**}\ln\left(\frac{\delta_x}{x_n(\varepsilon^{**})}\right)-\frac{\lambda_y}{\lambda_x}\varepsilon^*\ln\left(\frac{\delta_x}{x_n(\varepsilon^*)}\right)$$
$$=\frac{\lambda_y}{\lambda_x}\Delta\varepsilon\ln\left(\frac{\delta_x}{x_n(\varepsilon^{**})}\right)+\frac{\lambda_y}{\lambda_x}\varepsilon^*\left[\ln\left(\frac{\delta_x}{x_n(\varepsilon^{**})}\right)-\ln\left(\frac{\delta_x}{x_n(\varepsilon^*)}\right)\right]$$
$$\leqslant\frac{\lambda_y}{\lambda_x}\Delta\varepsilon\ln\left(\frac{\delta_x}{x_n(\varepsilon^*)}\right)$$

since $x_n(\varepsilon^{**})>x_n(\varepsilon^*)$. Therefore,

$$y_n(\varepsilon^{**})-y_n(\varepsilon^*)\leqslant(1+K_3\varepsilon^*)\{y_{n-1}(\varepsilon^{**})-y_{n-1}(\varepsilon^*)\}$$
$$+\Delta\varepsilon\left\{K_1+K_2\varepsilon^*+\frac{\lambda_y}{\lambda_{x'}}\ln\left(\frac{\delta_x}{x_n(\varepsilon^*)}\right)\right\}.$$

From these recursive relations,

$$y_{N_0}(\varepsilon^{**}) - y_{N_0}(\varepsilon^*) \leqslant (1 + K_3\varepsilon^*)^{N_0} \{ y_0(\varepsilon^{**}) - y_0(\varepsilon^*) \} + (1 + K_3\varepsilon^*)^{N_0 - 1} \Delta\varepsilon \sum_{n=1}^{N_0} \times \left\{ K_1 + K_2\varepsilon^* + \frac{\lambda_y}{\lambda_x} \ln\left(\frac{\delta_x}{x_n(\varepsilon^*)} \right) \right\}.$$

Note that

$$\sum_{n=1}^{N_0} \ln\left(\frac{\delta_x}{x_n(\varepsilon^*)} \right) \leqslant \sum_{n=1}^{N_0} \ln\left(\frac{\delta_x}{c_2 n\varepsilon^*} \right) \leqslant N_0 \ln\left(\frac{\delta_x}{c_2} \right) - (N_0 + 1) \ln(N_0 + 1) + (N_0 + 1) + N_0 \ln\left(\frac{1}{\varepsilon^*} \right)$$

Since $N_0 \asymp O(1/\varepsilon^*)$ and $y_0(\varepsilon^{**}) - y_0(\varepsilon^*) \leqslant c_3 \Delta\varepsilon$ for some $c_3 > 0$, it follows that

$$0 < y_{N_0}(\varepsilon^{**}) - y_{N_0}(\varepsilon^*) \leqslant \frac{C_1}{\varepsilon^*} \Delta\varepsilon$$

for some constant $C_1 > 0$.

Now suppose that $n > N_0$. We then define $p_n(\varepsilon)$ using the return map on the section Σ_P. In this case,

$$y_n(\varepsilon) - y_{n-1}(\varepsilon) = \varepsilon k(y_{n-1}(\varepsilon), \varepsilon), \tag{5.4}$$

where $k(y, \varepsilon) = -h(y, \varepsilon)$ which was defined in Subsection 4.4. Hence,

$$y_n(\varepsilon^{**}) - y_n(\varepsilon^*) = y_{n-1}(\varepsilon^{**}) - y_{n-1}(\varepsilon^*) + k(y_{n-1}(\varepsilon^{**}), \varepsilon^{**})\, \varepsilon^{**} - k(y_{n-1}(\varepsilon^*), \varepsilon^*)\, \varepsilon^*.$$

As before,

$$y_n(\varepsilon^{**}) - y_n(\varepsilon^*) \leqslant (1 + K_3'\varepsilon^*) \{ y_{n-1}(\varepsilon^{**}) - y_{n-1}(\varepsilon^*) \} + \Delta\varepsilon(K_1' + K_2'\varepsilon^*)$$

where $K_1' > 0$, K_2', and K_3' are constants independent of ε. Hence,

$$\begin{aligned} y_N(\varepsilon^{**}) - y_N(\varepsilon^*) &\leqslant (1 + K_3'\varepsilon^*)^{N-N_0}\{y_{N_0}(\varepsilon^{**}) - y_{N_0}(\varepsilon^*)\} \\ &\quad + (K_1' + K_2'\varepsilon^*)\,\Delta\varepsilon\{(1 + (1 + K_3'\varepsilon^*) \\ &\quad + \cdots (1 + K_3'\varepsilon^*)^{N-N_0-1}\} \\ &= (1 + K_3'\varepsilon^*)^{N-N_0}\{y_{N_0}(\varepsilon^{**}) - y_{N_0}(\varepsilon^*)\} \\ &\quad + (K_1' + K_2'\varepsilon^*)\,\Delta\varepsilon\,\frac{(1 + K_3'\varepsilon^*)^{N-N_0} - 1}{K_3'\varepsilon^*} \end{aligned}$$

Since $N - N_0 \asymp O(1/\varepsilon^*)$,

$$y_N(\varepsilon^{**}) - y_N(\varepsilon^*) \leqslant C_2(y_{N_0}(\varepsilon^{**}) - y_{N_0}(\varepsilon^*)) + C_3\frac{1}{\varepsilon^*}\Delta\varepsilon$$

with C_2 and C_3 both positive. In a similar fashion,

$$y_N(\varepsilon^{**}) - y_N(\varepsilon^*) \geqslant C_4(y_{N_0}(\varepsilon^{**}) - y_{N_0}(\varepsilon^*)) + C_5\frac{1}{\varepsilon^*}\Delta\varepsilon$$

with C_4, $C_5 > 0$. It follows that

$$C_5\frac{1}{\varepsilon^*}\Delta\varepsilon \leqslant y_N(\varepsilon^{**}) - y_N(\varepsilon^*) \leqslant (C_1C_2 + C_3)\frac{1}{\varepsilon^*}\Delta\varepsilon.$$

This completes the proof of (5.2).

6. APPENDIX

The dimensionless differential equations used for our numerical computations are

$$\frac{dv}{dt} = -\bar{g}_{Ca}m_\infty(v)(v-1) - \bar{g}_K w(v - v_K) - \bar{g}_L(v - v_L) + i$$

$$\frac{dw}{dt} = \phi(w_\infty(v) - w)\,\tau_w(v)$$

$$\frac{di}{dt} = \varepsilon(v_* - v - \alpha i)$$

where

$$m_\infty(v) = 0.5\left[1 + \tanh\left(\frac{v+0.01}{0.15}\right)\right]$$

$$w_\infty(v) = 0.5\left[1 + \tanh\left(\frac{v-0.1}{0.145}\right)\right]$$

$$\tau_w(v) = \cosh\left(\frac{v-0.1}{0.29}\right)$$

These equations were originally derived by Rinzel and Ermentrout [28] as a modification of a model due to Morris and Lecar [21]. The parameters for Fig. 1 are the following: $\bar{g}_{Ca} = 1.0$, $\bar{g}_K = 2.0$, $\bar{g}_L = 0.5$, $\phi = 1.15$, $v_K = -0.7$, $v_L = -0.5$, $\alpha = 0$, $v_* = -0.22$, and $\varepsilon = 0.002$.

ACKNOWLEDGMENTS

This research was supported in part by NSF Grant DMS-9423796.

REFERENCES

1. J. C. Alexander and D. Cai, On the dynamics of bursting systems, *J. Math. Biol.* **29** (1991), 405–423.
2. V. I. Arnold, "Ordinary Differential Equations," MIT Press, Cambridge, MA, 1973.
3. I. Atwater, C. M. Dawson, A. Scott, G. Eddlestone, and E. Rojas, The nature of the oscillatory behavior in electrical activity for pancreatic β-cell, *in* "Biochemistry and Biophysics of the Pancreatic β-Cell," pp. 265–284, Georg Thieme Verlag, New York, 1981.
4. R. Bertram, M. J. Butte, T. Kiemel, and A. Sherman, Topological and phenomenological classification of bursting oscillations, *Bull. Math. Biol.* **57** (1995), 413–439.
5. J. Carr, "Applications of Center Manifold Theory," Springer-Verlag, New York/Heidelberg/Berlin, 1981.
6. T. R. Chay and J. Keizer, Minimal model for membrane oscillations in the pancreatic beta-cell, *Biophys. J.* **42** (1983), 181–190.
7. T. R. Chay and J. Rinzel, Bursting, beating, and chaos in an excitable membrane model, *Biophys. J.* **47** (1985), 357–366.
8. E. J. Doedel, AUTO, a program for the automatic bifurcation and analysis of autonomous systems, *Congr. Numer.* **30** (1981), 265–284.
9. G. B. Ermentrout and N. Kopell, Parabolic bursting in an excitable system coupled with a slow oscillation, *SIAM J. Appl. Math.* **46** (1986), 233–253.
10. N. Fenichel, Persistence and smoothness of invariant manifolds for flows, *Indiana Univ. Math. J.* **21** (1971), 193–226.
11. N. Fenichel, Asymptotic stability with rate conditions, *Indiana Univ. Math. J.* **23** (1974), 1109–1137.
12. N. Fenichel, Asymptotic stability with rate conditions, II, *Indiana Univ. Math. J.* **26** (1977), 87–93.

13. N. Fenichel, Geometric singular perturbation theory for ordinary differential equation, *J. Differential Equations* **31** (1979), 53–98.
14. R. Fitzhugh, Impulses and physiological states in models of nerve membrane, *Biophys. J.* **1** (1961), 445–466.
15. J. Guckenheimer and P. J. Holmes, "Nonlinear Oscillations, Dynamical Systems, and Bifurcations of Vector Fields," Springer-Verlag, New York/Heidelberg/Berlin, 1983.
16. J. L. Hindmarsh and R. M. Rose, A model of neuronal bursting using three coupled first order differential equation, *Proc. Roy. Soc. London B* **221** (1984), 87–102.
17. M. W. Hirsch and C. C. Pugh, "Invariant Manifolds," Springer Lecture Notes in Mathematics, Vol. 583, Springer-Verlag, New York/Heidelberg/Berlin, 1977.
18. M. W. Hirsh and S. Smale, "Differential Equations, Dynamical Systems and Linear Algebra," Academic Press, New York, 1974.
19. A. L. Hodgkin and A. F. Huxley, A quantitative description of membrane current and its application to conduction and excitation in nerve, *J. Physiol. (London)* **117** (1952), 500–544.
20. E. F. Mishchenko and N. Kh. Rozov, "Differential Equations with Small Parameters and Relaxation Oscillations," Plenum Press, New York/London, 1975.
21. C. Morris and H. Lecar, Voltage oscillations in the barnacle giant muscle fiber, *Biophys. J.* **35** (1981), 193–213.
22. J. Nagumo, S. Aritomo, and S. Yoshizawa, An active pulse transmission line simulating nerve axon, *Proc. IRE* (1964), 2061–2070.
23. M. Pernarowski, R. M. Miura, and J. Kevorkian, Perturbation technique for models of bursting electrical activity in pancreatic β-cells, *SIAM J. Appl. Math.* **52** (1992), 1627–1650.
24. L. S. Pontryagin and L. V. Rodygin, Approximate solution of a system of ordinary differential equations involving a small parameter in the derivatives, *Izdat. Akad. Nauk SSSR Moscow* **3** (1956), 570.
25. L. S. Pontryagin and L. V. Rodygin, Periodic solution of a system of ordinary differential equations with a small parameter in the terms containing derivatives, I, *in* "Proceedings, Third All-Union Mathematical Conference, Moscow, June–July, 1956," Vol. 2, p. 93; II, *Izdat. Akad. Nauk SSSR, Moscow* **3** (1956), 570.
26. J. Rinzel, "Ordinary and Partial Differential Equations" (B. D. Sleeman and R. J. Jarvis, Eds.), pp. 304–316, Springer-Verlag, New York, 1985.
27. J. Rinzel, "Pro. Inter. Congress. of Math." (A. M. Gleason, Ed.), pp. 1578–1593, Amer. Math. Soc., Providence, 1987.
28. J. Rinzel and G. Ermentrout, Analysis of neural excitability and oscillations, *in* "Methods in Neural Modeling, from Synapses to Networks" (C. Koch and I. Seger, Eds.), pp. 135–169, MIT Press, Cambridge, MA, 1989.
29. J. Rinzel and Y. S. Lee, On different mechanism for membrane potential bursting, *in* "Lecture Notes in Biomathematics," Vol. 66, pp. 19–33, Springer-Verlag, New York/Heidelberg/Berlin, 1986.
30. P. Rorsman and G. Trube, Calcium and delayed potassium currents in mouse pancreatic β-cells under voltage-clamp conditions, *J. Physiol.* **374** (1986), 531–550.
31. A. Sherman, Contributions of modeling to understanding stimulus-secretion coupling in pancreatic β-cells, *Amer. J. Physiol.* **271** (1996), E362–E372.
32. A. Sherman, J. Rinzel, and J. Keizer, Emergence of organized bursting in clusters of pancreatic β-cells by channel sharing, *Biophys. J.* **54** (1988), 411–425.
33. J. Stoer and R. Bulirsch, "Introduction to Numerical Analysis," Springer-Verlag, New York/Heidelberg/Berlin, 1980.
34. P. Szmolyan, Transversal heteroclinic and homoclinic orbits in singular perturbation problems, *J. Differential Equations* **92** (1991), 252–281.

35. D. Terman, Chaotic spikes arising from a model for bursting in excitable membranes, *SIAM J. Appl. Math.* **51** (1991), 1418–1450.
36. D. Terman, The transition from bursting to continuous spiking in excitable membrane models, *J. Nonlinear Sci.* **2** (1992), 135–182.
37. A. N. Tihonov, On the dependence of the solutions of the differential equations on a small parameter, *Mat. Sb.* **31** (1948), 575–586.
38. X-J. Wang and J. Rinzel, Oscillatory and bursting properties of neurons, *in* "The Handbook of Brain Theory and Neural Networks" (M. A. Arbib, Ed.), pp. 686–691, MIT Press, Cambridge, MA, 1995.
39. S. Wiggins, "Global Bifurcations and Chaos: Analytic Methods," Springer-Verlag, New York/Heidelberg/Berlin, 1988.